Mg-corrosion, hydroxyapatite, and bone healing

Håkan Nygren[a)]
Department of Medical Chemistry and Cell Biology, Institute of Biomedicine, Sahlgrenska Academy, University of Gothenburg, POB 440, 40530 Gothenburg, Sweden

Narmin Bigdeli
Department of Clinical Chemistry and Transfusion Medicine, Institute of Biomedicine, University of Gothenburg, 40530 Gothenburg, Sweden

Lars Ilver
Department of Applied Physics, Chalmers University of Technology, 41296 Gothenburg, Sweden

Per Malmberg
Department of Chemistry and Chemical Engineering, Chalmers University of Technology, 41296 Gothenburg, Sweden

(Received 9 February 2017; accepted 11 April 2017; published 2 May 2017)

The different capacities of magnesium in the metallic form (Mg-metal) and magnesium oxide (MgO) to stimulate bone healing are possible clues in the search for products that may promote bone healing. Since both Mg-metal and MgO can be assumed to release comparable amounts of Mg^{2+} ions during their reactions in the tissue where they have been implanted, it is of some importance to follow this process and analyze the resulting mineral formation in the tissue at the implantation site. Implants of MgO were inserted into rat tibia, and the bone healing was compared with sham-operated controls. Samples were taken after 1 week of healing and analyzed by histology, environmental scanning electron microscopy equipped with an energy dispersive x-ray spectroscopy analyzer, and time-of-flight secondary ion mass spectrometry (ToF-SIMS). Callus bone was seen in sham-operated controls after 1 week of healing. Implantation of MgO impaired the callus bone formation by replacing bone with apparently mineralized areas, lacking osteocytes and were denoted, amorphous bodies. Elemental analysis showed increased levels of Ca (7.1%), P (3.7%), and Mg (0.2%) in the bone marrow of MgO-treated animals versus sham-operated controls Ca (2.4%), P (2.3%), and Mg (0.1%). The Ca content of the cortical bone was also significantly increased (Ca, 29% increase) in MgO-treated animals compared to sham-operated controls. The Ca content of the cortical bone of sham-operated animals was also significantly ($p < 0.05$) higher than the corresponding value of untreated animals, which means that the surgical trauma induces an altered composition of the bone mineral. The Ca/P ratio was 1.26–1.68, which is compatible with that of mineralized bone with different contents of organic materials. Analysis of bone sections using ToF-SIMS showed the presence of hydroxyapatite (HA) and $MgCO_3$ in the bone marrow and in cortical bone. Analysis using x-ray photoelectron spectroscopy of Mg, MgO, and $MgCO_3$ after incubation with cell culture medium (DMEM), *in vitro*, showed binding of $CaPO_4$ at the Mg and MgO samples. The Ca/P ratio was 0.8, indicating a higher P content than that expected for HA. Exposure of human embryonic stem cells to Mg species preincubated in DMEM resulted in HA production by the cells. Thus, two sources of $CaPO_4$ in the bone marrow of MgO-treated bone were defined, catalytic formation on Mg-species and synthesis from activated stem-cells. The presented data suggest that bone healing near Mg implants is congruent with the fracture healing of bone, boosted by high HA levels in the bone marrow. In this context, the different capacities of Mg-metal and MgO to catalyse the formation of HA can be important clues to their different bone promoting effects. *© 2017 Author(s). All article content, except where otherwise noted, is licensed under a Creative Commons Attribution (CC BY) license (http://creativecommons.org/licenses/by/4.0/).*
[http://dx.doi.org/10.1116/1.4982601]

I. INTRODUCTION

Magnesium implants have, since long, been known to stimulate bone formation *in vivo*.[1] The application of the metal as an implant material has been hampered by the formation of hydrogen gas during Mg corrosion.[2] The gas development in the tissue can be avoided by implanting Mg corrosion products, like MgO.[3] Implantation of MgO has been reported to stimulate bone formation, but the effect was intermittent and of short duration.[3] It meets with the difficulty in explaining the different effects of Mg-metal and MgO with differences in the levels of Mg-ions in the tissue. Magnesium implants corrode rapidly under physiological conditions, resulting in the production of MgO which is then

[a)]Electronic mail: hakan.nygren@gu.se

converted into more stable products, $Mg(OH)_2$ and $MgCO_3$.[4] The type of product formed during corrosion is dependent on the corrosion environment. For example, the presence of CO_2 resulted in the formation of $MgCO_3$ (Refs. 4 and 5) as the main corrosion product. Calcium phosphates, including hydroxyapatite (HA), precipitate on the surface of corroding Mg.[6,7] To gain a better understanding of the corrosion process and how it might facilitate mineralization *in vivo*, we applied energy dispersive x-ray spectroscopy (ESEM/EDX), ToF-SIMS, and XPS for chemical and elemental analyses of bone mineralization.[8–11] The importance of the MgO phase in HA formation has been reported.[9,12,13] Hence, Mg corrosion products may function as substrates facilitating the formation of low crystalline, carbonated HA (CHA), where the high Mg ion concentration inhibits its transition to crystalline HA.[14] Biological apatite is generally CHA. Amorphous or less crystalline CHA has been found to be more efficient in activating osteoblasts and may be more beneficial than synthetic HA for early bone ingrowth.[15]

Several studies have been carried out on Mg-metal and its corrosion, but little data are available on the effect of MgO on mineral formation *in vivo*. The present study was performed to elucidate the effects of calcium phosphates, formed by catalysis, on the surface of Mg corrosion products, on human embryonic stem cells (hESCs) *in vitro*, and on bone tissue *in vivo* when implanted into rat tibia.

II. EXPERIMENT

A. Sample preparation

Commercial pure granules of Mg, MgO, and $MgCO_3$ (99.9% pure, Sigma-Aldrich, Stockholm, Sweden) were incubated in cell culture medium (DMEM, Gibco-BRL/Invitrogen Gaithersburg, MD, Prod Nos. 11995-065 or 10829018) at 37 °C in a humified atmosphere with 5% CO_2 for 24–72 h, rinsed with saline (0.9% NaCl in water) and distilled water, and dry sterilized at 160 °C for 2 h. Single samples were used, and the experiments were repeated four times.

The chemical composition of the samples was analyzed by XPS and ToF-SIMS before and after incubation in DMEM. The surface composition was stable during incubation for 24–72 h in both the media used.

B. Human embryological stem cell culture

The hESC lines used in this study were SA167MFG-hESC and AS034.1MFG-hESC at passages 12 and 44, respectively, derived and characterized in a previous study.[16] Cell culturing was performed at the Department of Clinical Chemistry and Transfusion Medicine, Institute of Biomedicine, University of Gothenburg. Note that the stem cells were used adhere to plastic surfaces and can be cultured in polystyrene dishes.

C. Expansion of hESCs

In this study, hESCs were expanded and differentiated toward the osteogenic lineage directly onto tissue culture plastic without any supportive coating. In brief, cells were expanded in conditioned hES medium as described earlier[16] containing 80% KnockOut™ DMEM (Gibco-BRL/Invitrogen, pnr 10829018), 20% KnockOut serum replacement (Gibco-BRL/Invitrogen, 10828028), 2 mM L-glutamine (Gibco-BRL/Invitrogen, 25030-024), 0.1 mM β-mercaptoethanol (Gibco-BRL/Invitrogen 31350-010), and 1% nonessential amino acids (Gibco-BRL/Invitrogen, 11140-035) on Primaria® dishes (Falcon, surface modified polystyrene nonpyrogenic; Becton Dickinson, Franklin Lakes) and were incubated in a humidified atmosphere at 37 °C and 5% CO_2 (Heraeus BBD6220). The SA167MFG-hESC and AS034.1MFG-hESC were passaged every 4–6 days, and the medium was changed every second day.

D. Exposure of hESCs to MgO and $MgCO_3$ preincubated in DMEM

Undifferentiated hESCs were cultured on regular tissue culture plastic without predifferentiation stages such as embryoid body formation.

Cell exposure was performed by adding the preincubated MgO and $MgCO_3$ at a concentration of 5 or 0.5 mg/ml into the culture medium for 24 h. Each sample was made in triplicate, and the experiment was repeated three times. Samples of metal-Mg showed a very high increase in the *p*H and were omitted from this part of the study.

E. Von Kossa staining

Mineral production was studied using von Kossa staining performed by washing the cells with phosphate-buffered saline (PBS) followed by fixation in glutaraldehyde solution (25% in H_2O Sigma-Aldrich diluted 1:10) for 2 h. A solution of $AgNO_3$ (2% w/v: Sigma-Aldrich) was added, and the plates were kept in the dark for 10 min. The plates were then rinsed three times with distilled H_2O before being exposed to bright light for 15 min. After washing with distilled H_2O, samples were quickly dehydrated by adding 100% EtOH prior to microscopic inspection for mineralization as described earlier.[17]

F. Cell viability

hESCs were seeded onto a 24 well plate at a density of 10 000 cells/well. Cells were incubated in growth medium with or without the presence of metal oxides for 24 h to allow for attachment. The attached cells were considered viable and floating cells nonviable. The surface coverage of viable cells was better than 90% in all the experiments.

G. Animal surgery

All animal work was approved by the Gothenburg animal experiment ethical committee. The surgery was performed as described in a previous study,[18] shortly as follows. Male Sprague Dawley rats weighing 200 g (Charles River, Holland) were used. The animals were anesthetized with Isofluran (Baxter Medical CO, Kista, Sweden). A hole was drilled (drill d = 1 mm) in the tibial facies lateralis. Sterile

MgO powder was mixed with sterile saline into a paste (25% MgO dry weight), and 50 μl of the paste was implanted intramedullary. The paste was mixed with blood to create a fibrin matrix containing dispersed MgO granulae. Sham operated controls were left without the implant. The animals were kept at the Experimental Biomedicine facility and were fed commercial pellets and water ad libitum. The animals were harvested after 1 week by separating the heart from the main arteries, and the tibia bones were dissected.

H. Histology

Histology was made according to routine procedures. The samples were fixed with 1% paraformaldehyde in PBS for 3 days. The bone samples were then decalcified for 2 weeks in 0.15 M ethylenediaminetetraacetic acid tetrasodium dihydrate (Sigma-Aldrich® Sweden AB) containing 0.5% paraformaldehyde. The medium was changed every third day. The samples were then submitted to Histolab Products (Göteborg, Sweden), for preparation by dehydration in graded series of ethanol, and placed in xylene embedded in Histowax embedding medium at 60 °C. The samples were then cut, mounted on Superfrost Plus glass slides (Menzel-Gläser, Germany), stained with hematoxylin and eosin, and examined using a Zeiss Axioscope 2 microscope, equipped with an Axiocam ICc 1 digital camera (Zeiss, Jena, Germany).

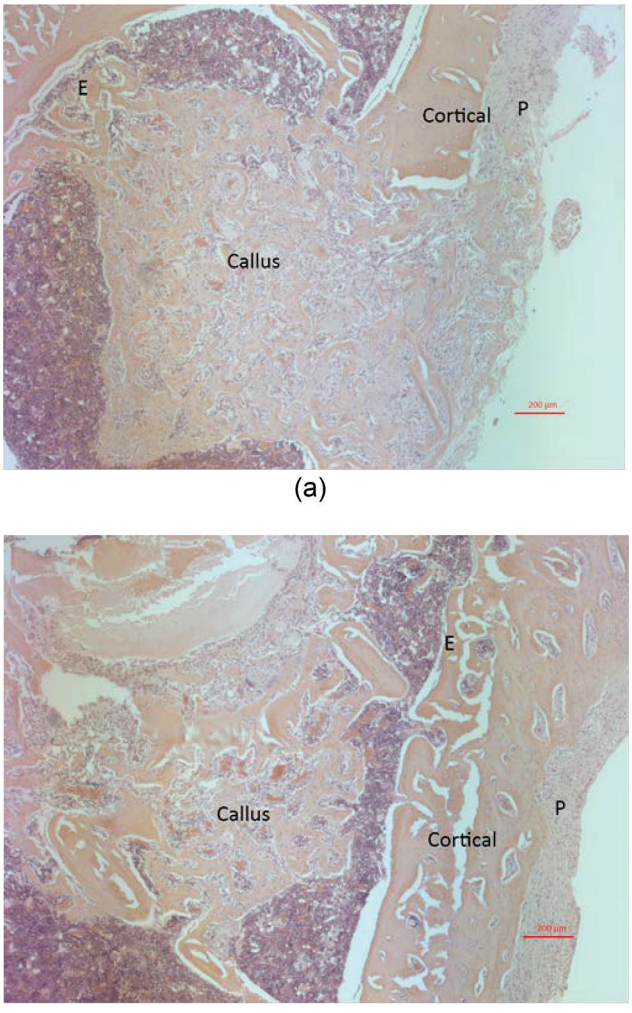

FIG. 1. (a) Sham-operated control 1 week. Light micrograph of a histological section of rat tibia after 1 week of healing after sham operation. Endosteum (E), periosteum (P) cortical bone, and normal callus bone are shown. (b) MgO 1 week. Light micrograph of a histological section of rat tibia after 1 week of healing after implantation of MgO in the bone marrow. Endosteum (E), periosteum (P) cortical bone, and callus bone are shown. The site of implantation of MgO is seen, together with amorphous bodies sorrounding the callus bone. The amount of callus bone is lower in the MgO-treated tibia than in sham-operated controls.

I. Environmental scanning electron microscopy and EDX

The samples were fixed by freeze-substitution which freezes ions *in situ* and substitutes water with absolute ethanol to avoid the dissolution of salts. The rat tibiae were immersed into absolute ethanol on dry ice. The bone tissue was substituted with alcohol for one week at −80 °C, warmed to room temperature, cut with a diamond saw, using absolute ethanol as the lubricating liquid, and rinsed carefully with absolute ethanol. The samples were left to dry at room temperature. An FEI Quanta 200 FEG ESEM operating at an accelerating voltage of 20 kV was used for imaging and chemical analysis. All images were acquired in the backscattered electron imaging mode at a pressure of 1 Torr in the low vacuum region in order to avoid charging effects. EDX data were recorded using an Oxford EDX detector, and spectra were evaluated using the INCA software. Analysis of spots was used to get the maximum resolution and sensitivity. The results were expressed as mass % of all the detected elements or atom % for the calculation of the Ca/P ratio.

J. ToF-SIMS

ToF-SIMS analysis was performed with a TOF.SIMS 5 instrument (ION-TOF GmbH, Münster, Germany) using a Bi_3^+ cluster ion gun as the primary ion source. Multiple (n = 5) regions ranging from 100 × 100 to 500 × 500 μm were analyzed using a pulsed primary ion beam (Bi_3^+, 0.34 pA at 25 keV) with a focus of approximately 2 μm and a mass resolution of M/ΔM = 5000 fwhm at m/z 500. All the spectra were acquired and processed using the Surface Lab software (version 6.4, ION-TOF GmbH, Münster, Germany), and the ion intensities used for calculations were normalized to the total ion dose of each measurement. ToF-SIMS analysis is surface sensitive and detects atoms and

TABLE I. Content of Ca, P, and Mg (mass %) in sham-operated bone (n = 4).

Element (mass %)	Sham bone marrow	Sham IM mineral	Sham cortical bone
Ca	2.37 ± 0.32	19.29 ± 1.91	21.05 ± 0.92
P	2.27 ± 0.27	11.44 ± 0.49	12.04 ± 0.43
Mg	0.08 ± 0.018	0.45 ± 0.038	0.42 ± 0.046

TABLE II. Content of Ca, P, and Mg (mass %) in MgO-implanted bone (n = 4).

Element (mass %)	MgO bone marrow	MgO IM mineral	MgO cortical bone
Ca	7.08 ± 1.74	19.3 ± 1.97	27.1 ± 3.3
P	3.66 ± 0.52	11.79 ± 2.84	12.08 ± 0.61
Mg	0.19 ± 0.04	0.43 ± 0.11	0.45 ± 0.07

molecules in the first nanometer at the surface. ToF-SIMS is a qualitative analysis of molecular species.

K. XPS

XPS was also used for similar untreated and DMEM-incubated samples to characterize the changes in surface chemistry. The XPS spectra were recorded with a PHI 5000 System (Physical electronics, Chanhassen, Ma, USA) using monochromatized Al Ka radiation (hv¼ 1486.6 eV) as the x-ray source, and the photoelectron take-off angle was set at 45. Atomic sensitivity factors for quantitative analysis were taken from Ref. 19. The binding energies were corrected according to the C1*s* peak with CH_2 (284.6 eV) as the standard.

L. Statistical analysis

Statistical analysis was performed using the t-test. The limit of statistical significance was set at $p > 0.05$. Each leg was considered a statistical unit.

III. RESULTS AND DISCUSSION

The trauma of drilling a defect in the compact bone of rat tibia results in the formation of callus bone within the first week of healing.[20] In the present study, callus bone was seen in histological samples of the bone drill-defect of sham-operated controls after 1 week of healing [Fig. 1(a)]. The effect of implantation of MgO on bone healing was analyzed by light microscopy and ESEM. In MgO-treated bone [Fig. 1(b)], callus bone tissue was seen together with apparently mineralized areas, lacking osteocytes and were denoted, amorphous bodies. The periosteum was hypertrophic in both MgO-treated and sham-operated bones. Thus, implantation of 50 μl of 10% MgO-paste in a drilled hole in rat tibia followed by healing for 1 week decreases the amount of callus bone formed and causes the formation of amorphous bodies (Fig. 1).

In order to analyze the elemental composition of the amorphous bodies, bone was freeze-substituted in order to preserve the mineral content, cut into sections, dried, and analyzed by ESEM/EDX in the electron backscattering mode.

Images of rat tibia obtained using ESEM in the backscattering electron mode show the mass contrast in the tissue. High intensity (white) reveals the area containing elements with a high atomic number, and dark areas contain elements of lower atomic numbers. Tibia sections from sham-operated rats show healing of the drill-defect by lamellar callus bone in the bone marrow cavity (IM mineral) after 1 week of healing. Sections from tibia of rats receiving MgO-implants show higher intensity of backscattering from lammellar

TABLE III. Content of Ca, P, and Mg (mass %) in untreated rat tibia bone (n = 4).

Element (mass %)	Untreated bone marrow	Untreated cortical bone
Ca	2.41 ± 0.63	18.25 ± 1.17
P	2.57 ± 0.79	10.63 ± 0.49
Mg	0.12 ± 0.02	0.42 ± 0.05

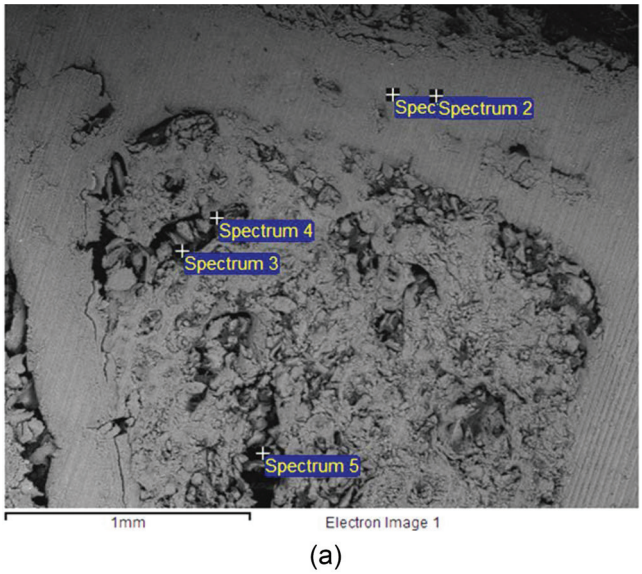

(a)

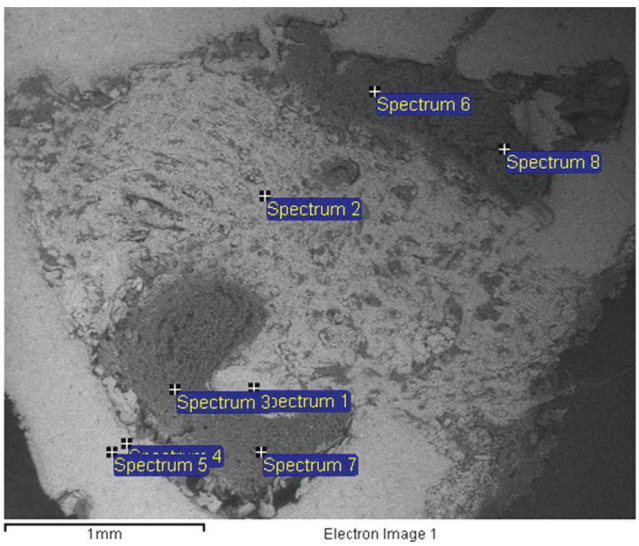

(b)

FIG. 2. (a) ESEM image of the rat tibia section after 1 week of healing after implantation of MgO. EDX analysis was made at the marked spots, representing cortical bone, bone marrow, and mineral lamellae of callus bone. Spectra 1 and 2 were taken from compact bone. Spectra 3 and 5 were taken from unmineralized bone marrow. (b) ESEM image of the rat tibia section after 1 week of healing after sham operation. EDX analysis was made at the marked spots, representing cortical bone (spectra 4 and 5), bone marrow, (spectra 3 and 6) and callus bone (spectrum 2).

mineral, in the bone marrow cavity (IM mineral) with a more irregular structure than callus bone seen in controls. The statistical evaluation ($n = 4$) of EDX data from tibia of sham-operated and MgO-implanted rats, after 1 week of healing, is shown in Tables I–III.

A statistically significant difference was found in the Ca, P, and Mg content in the soft tissue of the bone marrow of sham-operated animals versus the soft tissue of the bone marrow of MgO-treated animals ($p \leq 0.05$). The difference in the Ca content of sham-operated or untreated cortical bone versus the Ca content of MgO-treated cortical bone was statistically significant ($p < 0.05$). The difference in Ca levels between sham-operated controls and untreated animals was also statistically significant ($p < 0.05$). Thus, the presented data suggest that implantation of MgO in bone marrow causes elevated levels of Ca, P, and Mg in the soft tissue of the bone marrow and increased levels of Ca, but not of P and Mg, in the cortical bone. The surgical trauma in itself also causes an alteration of the mineral composition of the cortical bone detected as increased Ca-levels.

The Ca/P ratio (atomic %) of the calcium phosphate in the bone marrow was 1.29 and 1.26, respectively, for the sham-operated and MgO-treated bones. The Ca/P ratio of cortical, untreated bone was 1.32, for cortical sham-operated bone, the value was 1.35, and for cortical bone from MgO-treated animals, the Ca/P ratio was 1.68. The data show that different amounts of organic species are present at the different locations and that MgO-treatment increases the hydroxyapatite content of the cortical bone (Fig. 2).

Now, ToF-SIMS analyses were performed in order to elucidate the molecular species containing Ca, P, and Mg. Imaging mass spectrometry images of sections of rat tibia are shown in Figs. 3 and 4. The mineralized bone marrow after 1 week of healing of MgO-treated bones is shown in Fig. 3.

The total intensity of positively charged secondary ions is shown in Fig. 3(i). The secondary ion, representing the

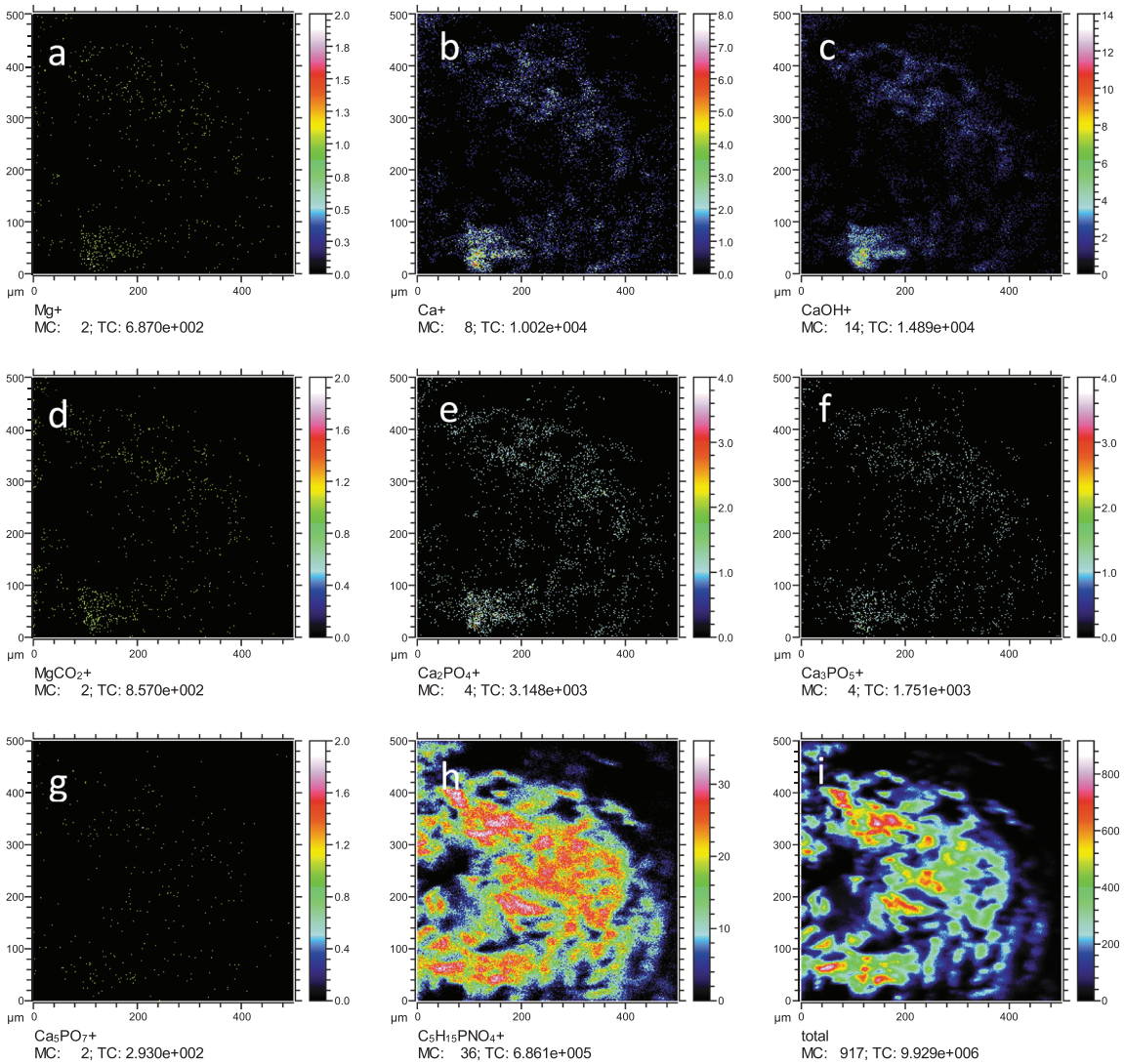

FIG. 3. Positive ion mode images the near implant soft tissue in rat tibia analyzed after 1 week of healing, showing the distribution of signals from (a) Mg^+, (b) Ca^+, (c) CaOH, (d) $MgCO_2^+$, (e) $Ca_2PO_4^+$, (f) $Ca_3PO_5^+$, and (g) $Ca_5PO_7^+$, (h) PC-head group, and (i) total ion image. Total dose density: 1.95×10^{11} ions/cm^2.

headgroup of phosphatidyl choline, is shown in Fig. 3(h) which shows the distribution of cell membrane lipids in the sample. Figure 3(a) shows the distribution of Mg^+, apparently in the form of $MgCO_2^+$ as can be seen in Fig. 3(d). Secondary ions stemming from Ca and $Ca(OH)_2$ can be seen in Figs. 3(b) and 3(c), and ions derived from HA are seen in Figs. 3(e)–3(g).

The cortical bone after 1 week of healing of MgO-treated bones is shown in Fig. 4. The total ion image in Fig. 4(i) shows the overall positive secondary ion distribution. The intensity and distribution of Mg^+ and $MgCO_2^+$ as seen in Figs. 4(a) and 4(d) in the cortical bone suggest that Mg^+ originates from more sources than $MgCO_3$. Ions originating from HA are also seen in Figs. 4(e)–4(g) as well as ions from Ca and $Ca(OH)_2$ in Figs. 4(b) and 4(c); all ions evidence the presence of hydroxyapatite in the bone marrow with a similar structure to cortical bone.

In order to elucidate the mechanism of HA formation in the bone marrow of MgO-treated animals, two sets of experiments were carried out in reduced systems: The first by incubating Mg, MgO, and $MgCO_3$ in cell culture fluid and analyzing the Ca, P, and C content of the Mg and its corrosion products and the second by incubating the Mg-species incubated in culture medium with human embryonic stem cells and analyzing the synthesis of hydroxyapatite by the cells. Similar *in vitro* systems have been used by others.[6,7,21]

The results of XPS-analysis of Mg, MgO, and $MgCO_3$ after incubation for 72 h in tissue culture medium are shown in Fig. 5.

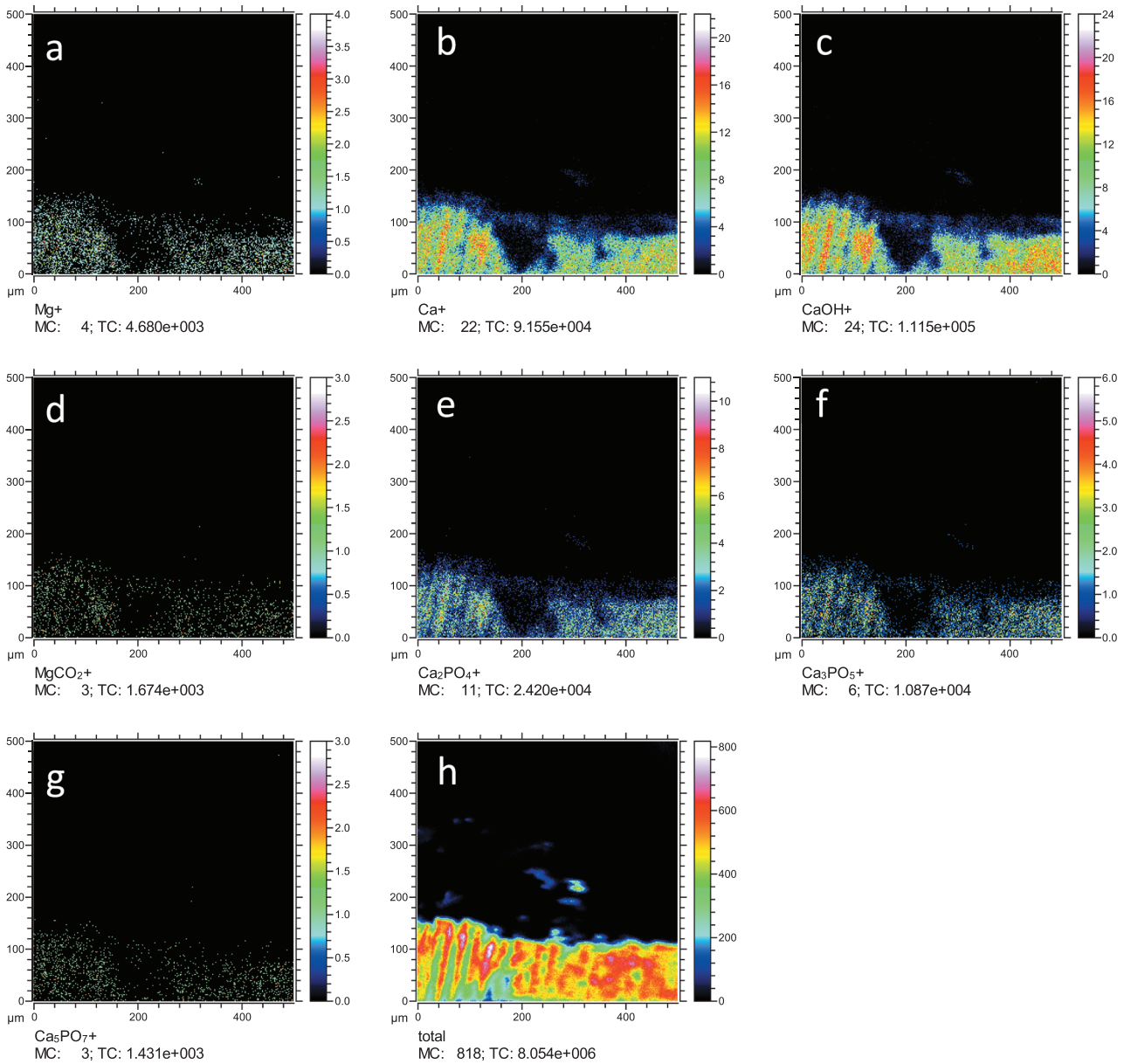

FIG. 4. Positive ion mode images the MgO implant surface implanted in rat tibia analyzed after 1 week of healing, showing the distribution of signals from (a) Mg^+, (b) Ca^+, (c) $CaOH^+$, (d) $MgCO_2^+$, (e) $Ca_2PO_4^+$, (f) $Ca_3PO_5^+$, and (g) $Ca_5PO_7^+$ and (h) the total ion image. Total dose density: 1.67×10^{11} ions/cm^2.

The intensity of the Ca 2s peak [Fig. 5(a)] is the highest for the Mg-samples and lower for the MgO-sample and shows background values for the $MgCO_3$-sample. The intensity of the P 2s peak [Fig. 5(b)] is the highest for the Mg samples and lower for the MgO sample and shows background values for the $MgCO_3$ sample. The Ca/P ratio is 0.8 on the Mg-sample and 0.79 on the MgO-sample, indicating that the calcium phosphates formed are not pure HA. This is consistent with the findings of Wagener and Virtanen,[6] showing that a mixture of calcium phosphates is formed on corroding Mg, including HA, after incubation in tissue culture medium. The formation of calcium phosphates on corroding Mg is apparently connected to the corrosion process rather than to the single corrosion products analyzed in the present study.

The results of exposing hESCs to Mg, MgO, and $MgCO_3$ that have been preincubated in MEM for 24–72 h are shown in Fig. 6.

The hESCs, adhered to petri dishes and exposed to 5 mg/ml of preincubated MgO, showed signs of losing adhesion which is a cytotoxicity reaction. Approximately 25% of the cells were lost at this concentration of MgO. At a tenfold lower concentration, the cells were seen adhering to the dishes [Figs. 6(a) and 6(b)]. Staining the fixed cultures with von Kossa staining showed that the cells produced HA after

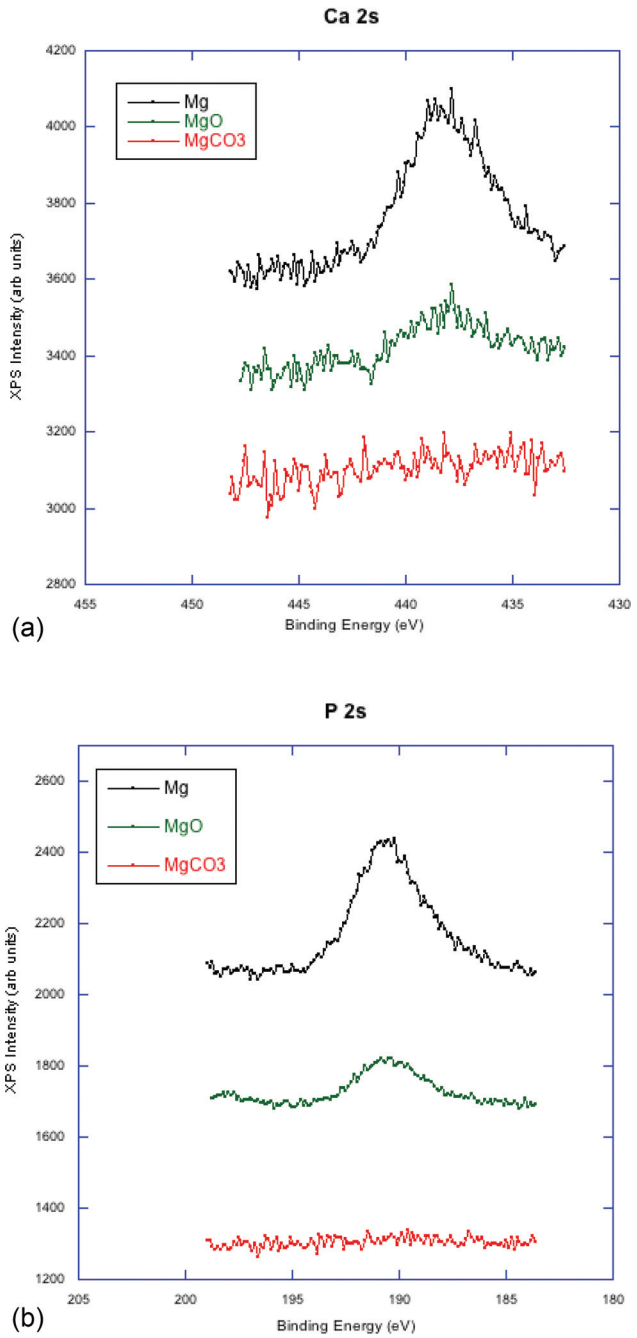

FIG. 5. (a) XPS intensity of the Ca 2s peak from Mg, MgO, and $MgCO_3$ after incubation for 72 h in DMEM, rinsing three times with distilled water, and air drying. (b) XPS intensity of the P 2s peak from Mg, MgO, and $MgCO_3$ after incubation for 72 h in DMEM, rinsing three times with distilled water, and air drying.

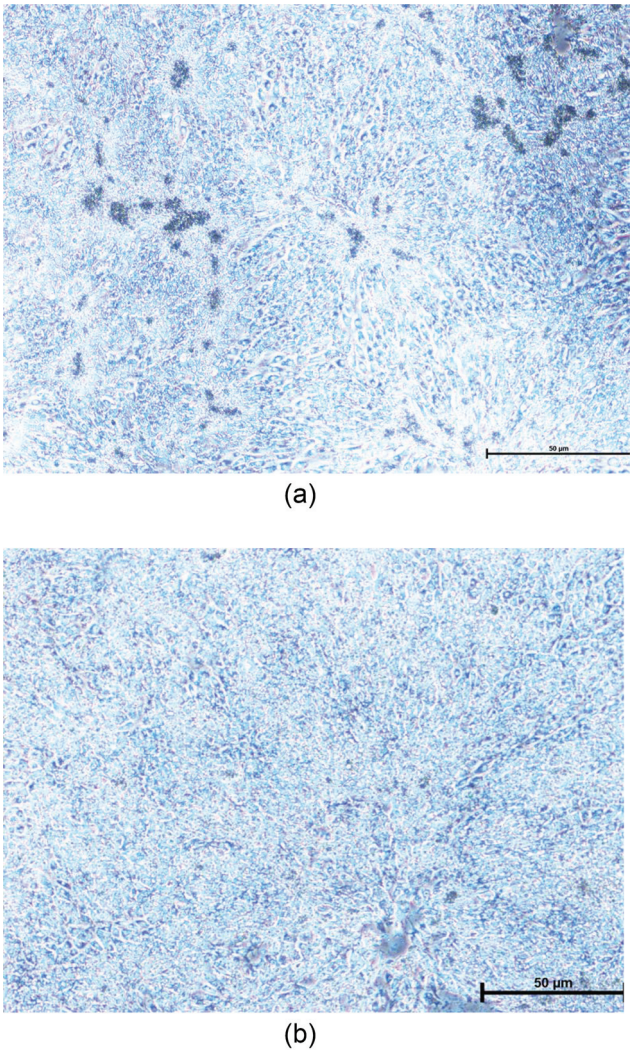

FIG. 6. (a) Human embryonic stem cells (ASO34 1MFG) grown for 24 h exposed to 0.5 mg/ml of MgO preincubated in DMEM. Von Kossa staining reveals precipitate of HA in the extracellular space. The surface coverage of adhered cells is >90%. (b) Human embryonic stem cells (ASO34 1MFG) grown for 24 h exposed to 0.5 mg/ml of $MgCO_3$ incubated in DMEM. Von Kossa staining shows minor, faintly stained precipitates. The surface coverage of adhered cells is >90%.

exposure to this concentration of MgO but not after exposure to $MgCO_3$, preincubated with DMEM. The cell reaction may either be a specific activation of the cells or a stress reaction at exposure to subtoxic levels of MgO. The *p*H of the growth medium was stable after exposure to MgO and $MgCO_3$, preincubated with DMEM. Incubation with corroding Mg increased the *p*H of the cell cultures (not shown).

The difference found between the Ca/P ratio *in vivo* by EDX analysis and the corresponding value for Mg and MgO incubated in DMEM *in vitro* indicates the importance of the cellular synthesis of HA also *in vivo*. Since $MgCO_3$, with a low level of $CaPO_4$ coating, also induced low levels of HA synthesis in hESCs and exposure to $MgCO_3$ fails to induce HA-synthesis in the stem cells, it is unlikely that Mg-ions are the cell activating agents. This finding is in accord with the results reported by Burmeister *et al.*,[20] showing a lack of specific stimulation of stem cells by Mg-ions. More likely, the cells respond to the mineral coating on the Mg-species.[20]

The increase in the mineral content of the cortical bone in MgO-treated rat tibia can be explained via a mechanism recently presented by Zhang *et al.*,[22] where implantation of Mg in rat bone was shown to activate calcitonin gene-related polypeptides via Substance P neurons. Nociceptors, the activation of which causes Substance P release, are also known[23] to be activated by heat and mechanical stimulation and are chemosensitive (for example, high *p*H). The data presented here suggest that increased bone mineralization is also seen after surgical trauma, known to activate nociceptors.

IV. SUMMARY AND CONCLUSION

MgO implanted in the bone marrow of rat tibia for 1 week induces the formation of high levels of hydroxyapatite in the bone marrow cavity. The levels of Ca, P, and Mg increase in the unmineralized soft tissue. The Ca levels increase in the cortical bone of sham-operated controls versus untreated animals and in the cortical bone of MgO-treated animals versus sham-operated controls. Thus, both the surgical trauma and the MgO-implant induce an altered mineral composition of the cortical bone. The activation of nociceptors is a possible mechanism of these effects. During incubation of Mg-metal and MgO in cell culture medium, Mg-metal is more efficient in catalyzing the formation of HA than MgO and $MgCO_3$. Human embryological stem cells grown in the presence of MgO, preincubated with cell culture medium, were activated and synthesized hydroxyapatite after 24 h in culture. Similar results have been published by others for Mg-metal.[20] The results of the present study define two sources of hydroxyapatite formation induced by MgO, binding to the MgO and activation of cells. A possible mechanism of stimulation of mineralization is via nociceptors.

ACKNOWLEDGMENT

The generous, long term financial support from Elos Medtech AB is gratefully acknowledged.

[1]F. Witte, Acta Biomater. **6**, 1680 (2010).
[2]A. A. Zierold, Arch. Surg. **9**, 365 (1924).
[3]C. Janning *et al.*, Acta Biomater. **6**, 1861 (2010).
[4]R. Willumeit, J. Fischer, F. Feyerabend, N. Hort, U. Bismayer, S. Heidrich, and B. Mihailova, Acta Biomater. **7**, 2704 (2011).
[5]R. Harrison, D. Maradze, S. Lyons, Y. F. Zheng, and Y. Liu, Prog. Nat. Sci. **24**, 539 (2014).
[6]V. Wagener and S. Virtanen, Mater. Sci. Eng., C **63**, 341 (2016).
[7]N. A. Agha, F. Feyerabend, B. Mihailova, S. Heidrich, U. Bismayer, and R. Willumeit-Romer, Mater. Sci. Eng. **58**, 817 (2016).
[8]A. Henss, M. Rohnke, T. El Khassawna, P. Govindarajan, G. Schlewitz, C. Heiss, and J. Janek, J. R. Soc. Interface **10**, 332 (2013).
[9]F. Witte, V. Kaese, H. Haferkamp, E. Switzer, A. Meyer-Lindenberg, C. J. Wirth, and H. Windhagen, Biomaterials **26**, 3557 (2005).
[10]H. B. Lu, C. T. Campbell, D. J. Graham, and B. D. Ratner, Anal. Chem. **72**, 2886 (2000).
[11]P. Malmberg, U. Bexell, C. Eriksson, H. Nygren, and K. Richter, Rapid Commun. Mass Spectrom. **21**, 745 (2007).
[12]Z. J. Li, X. N. Gu, S. Q. Lou, and Y. F. Zheng, Biomaterials **29**, 1329 (2008).
[13]B. Li, Y. Han, and K. Qi, ACS Appl. Mater. Interfaces **6**, 18258 (2014).
[14]H. C. Ding, H. H. Pan, X. R. Xu, and R. K. Tang, Cryst. Growth Des. **14**, 763 (2014).
[15]H. Nagai *et al.*, J. Mater. Sci.: Mater. Med. **26**, 99 (2015).
[16]N. Bigdeli, M. Andersson, R. Strehl, K. Emanuelsson, E. Kilmare, J. Hyllner, and A. Lindahl, J. Biotechnol. **133**, 146 (2008).
[17]T. Tallheden, J. E. Dennis, D. P. Lennon, E. Sjogren-Jansson, A. I. Caplan, and A. Lindahl, J. Bone Jt. Surg. Am. **85**A, 93 (2003).
[18]H. Nygren, M. Chaudhry, S. Gustafsson, G. Kjeller, P. Malmberg, and K. E. Johansson, J. Funct. Biomater. **5**, 158 (2014).
[19]*Auger, X-ray Photoelectron Spectroscopy*, edited by D. Briggs and M. P. Seah (Wiley, New Jersey, 1990).
[20]C. Eriksson, K. Ohlson, K. Richter, N. Billerdahl, M. Johansson, and H. Nygren, J. Biomed. Mater. Res. **83A**, 1062 (2007).
[21]A. Burmeister, R. Willumeit-Römer, and F. Feyerabend, J. Biomed. Mater. Res., Part B **105**, 165 (2017).
[22]Y. Zhang *et al.*, Nat. Med. **22** 1160 (2016).
[23]M. Wooten *et al.*, Nat. Commun. **5**, 4122 (2014).